Cerebral Cortex, 2018; 1–12

doi: 10.1093/cercor/bhy210
Original Article

ORIGINAL ARTICLE

In Vivo Femtosecond Laser Subsurface Cortical Microtransections Attenuate Acute Rat Focal Seizures

Shivathmihai Nagappan[1], Lena Liu[1], Robert Fetcho[1], John Nguyen[1], Nozomi Nishimura[1], Ryan E. Radwanski[1,2], Seth Lieberman[1], Eliza Baird-Daniel[2], Hongtao Ma[2,3], Mingrui Zhao[2,3], Chris B. Schaffer[1] and Theodore H. Schwartz[2,3,4]

[1]Meinig School of Biomedical Engineering, Cornell University, Ithaca, NY 14853, USA, [2]Department of Neurological Surgery, Weill Cornell Medicine of Cornell University, 525 East 68th Street, Box 99, New York, NY 10065, USA, [3]Brain and Mind Research Institute, Weill Cornell Medicine of Cornell University, New York Presbyterian Hospital, New York, NY 10021, USA and [4]Department of Neurological Surgery, Sackler Brain and Spine Institute, Weill Cornell Medicine of Cornell University, New York Presbyterian Hospital, New York, NY 10021, USA

Address correspondence to Mingrui Zhao, Department of Neurological Surgery, Weill Cornell Medicine of Cornell University, 525 East 68th Street, Box 99, New York, NY 10065, USA. Email: miz2003@med.cornell.edu; Chris B. Schaffer, Meinig School of Biomedical Engineering, Cornell University, B57 Weill Hall, Ithaca, NY 14853, USA. Email: cs385@cornell.edu; Theodore H. Schwartz, Department of Neurological Surgery, Weill Cornell Medicine of Cornell University, 525 East 68th Street, Box 99, New York, NY 10065, USA. Email: schwarh@med.cornell.edu

Shivathmihai Nagappan and Lena Liu contributed equally to this study

Abstract

Recent evidence shows that seizures propagate primarily through supragranular cortical layers. To selectively modify these circuits, we developed a new technique using tightly focused, femtosecond infrared laser pulses to make as small as ~100 μm-wide subsurface cortical incisions surrounding an epileptic focus. We use this "laser scalpel" to produce subsurface cortical incisions selectively to supragranular layers surrounding an epileptic focus in an acute rodent seizure model. Compared with sham animals, these microtransections completely blocked seizure initiation and propagation in 1/3 of all animals. In the remaining animals, seizure frequency was reduced by 2/3 and seizure propagation reduced by 1/3. In those seizures that still propagated, it was delayed and reduced in amplitude. When the recording electrode was inside the partially isolated cube and the seizure focus was on the outside, the results were even more striking. In spite of these microtransections, somatosensory responses to tail stimulation were maintained but with reduced amplitude. Our data show that just a single enclosing wall of laser cuts limited to supragranular layers led to a significant reduction in seizure initiation and propagation with preserved cortical function. Modification of this concept may be a useful treatment for human epilepsy.

Key words: 2-photon imaging, 4-aminopyridine, epilepsy model, laser, microsurgery

Introduction

Epilepsy is a neurological disorder involving recurrent seizures that affects 2.8% of the total population (Kobau et al. 2012; Kramer and Cash 2012), resulting from an imbalance between the excitatory and inhibitory connections in the cortex (Ribak et al. 1979; Treiman 2001). Patients with epilepsy can be broadly

divided into generalized or focal etiology (Benbadis 2001). In all epilepsies, first line therapy involves anticonvulsant medication but when these fail to control seizures, which occurs up to 30% of the time, surgical intervention is considered (Duncan et al. 2006). Surgical options include curative procedures, namely, removal of the epileptic focus, and palliative procedures involving neuromodulation of the abnormal circuitry.

The major impediment to surgical removal of the epileptic focus is disruption of normal cortical processing resulting in neurological impairments, which limits surgical cases to areas of the brain considered noncritical. Epileptic seizures are believed to initiate in layer 5 and propagate horizontally through layers 2–3 (Telfian and Connors 1998; Rheims et al. 2008; Wenzel et al. 2017), while cortical processing involves vertical columns of integrated circuitry (Mountcastle 1997) Almost 30 years ago, a surgical procedure called multiple subpial transections (MST) was devised by Morrell et al. (1989). This procedure involves creating several 1 cm spaced cuts through the entire thickness of gray matter with a blunt curved needle by hand with the goal of preventing the lateral horizontal spread of seizures, while maintaining pial blood supply to isolated cortical columns and preserving white matter connections. However, manual implementation of this technique resulted in marked variation in the size and orientation of the transections, ultimately causing significant damage to the adjacent cortex, but with limited seizure control and considerable impairments in normal brain function (Devinsky et al. 1994; Kaufmann et al. 1996; Schramm et al. 2002; Chang and Lowenstein 2003; Pondal-Sordo et al. 2006). For this reason, MSTs have been largely abandoned, in spite of the valid theoretical rationale, based mostly on inadequate technical implementation.

The first goal of this current study was to improve on both the spatial resolution and selectivity of MSTs while reduce the collateral damage. The second goal was to assess the efficacy of limited transections through the horizontal connections that exist in supragranular layers in attenuating seizure propagation while minimizing any collateral damage and impact on normal cortical function. In order to improve on the MST concept, we firstly developed a method for using tightly focused femtosecond pulses as a light scalpel to make subsurface incisions at varying lengths and depths in in vivo rodent brain. Femtosecond ablation results in highly localized damage as small as 100 μm in diameter since the threshold intensity is only reached at the laser's focus (Nguyen et al. 2011). We used this technique to create a 3D, "box-shaped" wall of continuous vertical cuts surrounding an acute epileptic focus, extending from the top of layer 2 to the bottom of layer 4 (DeFelipe et al. 2002) (Fig. 1A–D). We find that our femtosecond laser transections not only dramatically reduce propagation but also the initiation of seizure activity while preserving somatosensory responses elicited by tail stimulation. These results indicate that limited computer-driven supragranular subsurface femtosecond laser microtransections may be a promising treatment for focal human epilepsy.

Materials and Methods

Animal Preparation

All experimental procedures were approved by the Weill Cornell Medical College and Cornell University's Institutional Animal Care and Use Committee following NIH guidelines. Adult male Sprague Dawley rats (250–500 g) were induced with isoflurane (3–4%) in 100% O_2 by facemask. After induction, the

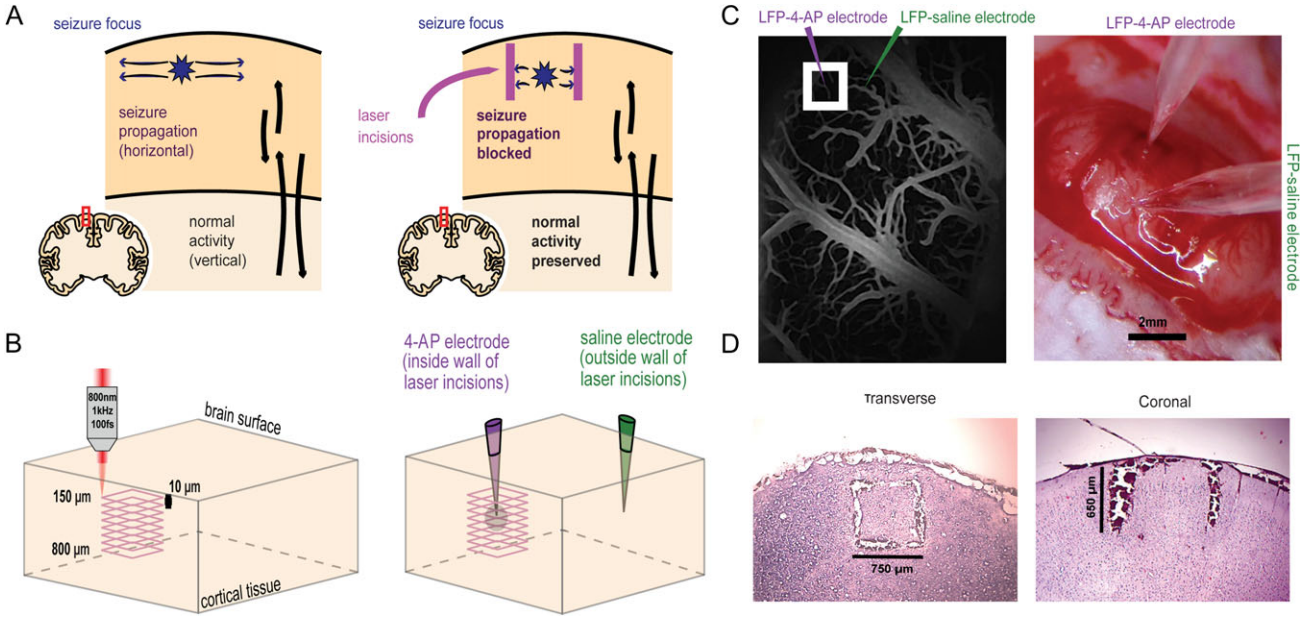

Figure 1. Femtosecond laser microtransections create a subsurface 3D cube to isolate the seizure focus. (*A*) Epileptic seizures primarily propagate horizontally in the cortex while columnar cortical activity primarily employs vertical connections (left). Laser incisions producing a 4-sided wall spanning cortical layers II–IV can block seizure propagation while preserving some vertical transmission of information (right). (*B*) Tightly focused, infrared wavelength, femtosecond laser pulses are programmed to make 65 overlaying square incisions beginning at 800 μm and ending 150 μm below brain surface. (*C*) In vivo 2-photon excited fluorescence imaging is used to visualize surface vasculature and make the laser incisions (left). 4-AP/LFP and LFP-saline electrodes are positioned by viewing the laser incisions using a light microscope (right). (*D*) Postmortem histological slices show the anatomical of the laser microtransections. Representative transverse slice through the 3D, box-shaped wall of laser incisions in which the 4 sides of the cut are evident (left). Representative coronal slice through the laser incision in which the full depth of the cuts is evident (right).

animal was maintained under isoflurane anesthesia using a small mask at 2–2.5%. A ~4×5 mm^2 cranial window was opened over one hemisphere between lambda and bregma to expose the neocortex. The dura was carefully removed. The brain was kept moist using artificial cerebrospinal fluid.

Femtosecond Laser Microtransections

Detailed description of the relationship between laser power, efficacy, width and adjacent tissue destruction of the femtosecond microtransections was presented in a prior paper (Nguyen et al. 2011). The beam from the ablation laser (Coherent: Legend 1k USP pumped by Coherent: Evolution 15 and seeded by Kapteyn-Murnane Laboratories: Chinhook Ti:Sapphire Laser, 50-fs pulses; 800-nm wavelength; 1-kHz repetition rate; pulse energies up to 0.5 mJ) was overlapped with the beam from the imaging laser. The imaging stage was moved so that the ablation beam would be focused 800 μm below the brain surface. The movement of the stage and the power of the laser was controlled by custom Matlab software. In order to isolate the seizure focus from all supragranular horizontal axonal and dendritic connections, we needed to fully circumscribe the focus and thus created a box-shaped cut around the 4-AP electrode. Using intervals of 10 μm, starting at 800 μm and ending at 150 μm below the brain surface, a planar square laser incision was created on 4 sides, resulting in a partially isolated cube (without top or bottom), or more precisely a column, with a height of 650 μm (Fig. 1B). The length of each transaction was set at 750 μm resulting in a partially isolated cube of ~0.366 mm^3. Given the known depths of each cortical layer in the rat, layers II–IV span from 123 to 732 μm in the rat indicating our cuts fully transected these layers (DeFelipe et al. 2002). Additionally, the custom Matlab program decreased the power of the ablation laser as the cuts were being made closer and closer to the brain surface according to an equation that relates depth of cut to laser power (Nguyen et al. 2011). This is because at greater depths, a higher power is needed to overcome the effects of scattering and create the same amount of damage (Helmchen and Denk 2005; Nguyen et al. 2011). At 800 μm, 32–35 mW and at 150 μm, 2–4 mW of laser power was used to create the incisions.

In Vivo 2-Photon Fluorescence Imaging

The animals were prepared for in vivo imaging. High molecular weight dextran conjugated with Fluorescein isothiocyanate was injected intravenously into the tail to fluorescently label the vasculature. An 8 mm cover slip was placed over the exposed brain. A 4× objective (Olympus, 4×, NA: 0.28) was used first to produce a wide-field image of the surface vasculature, and then a 20× objective (Olympus, 20×, NA: 0.95) was used to image the smaller vessels more precisely. Using the vascular roadmap, the 20× objective was positioned over a location in the brain to avoid large surface vessels so the laser transections would not damage the vessels (Fig. 1C).

Electrophysiology and Ictogenesis

Once the microtransections were completed, data acquisition proceeded after a 0.5-h delay. Ictal discharges were induced by injecting 0.5 μL 4-aminopyridine (4-AP, 25 mM, Sigma) using a Nanoject injector (Drummond) (Schwartz and Bonhoeffer 2001; Zhao et al. 2009). A faint outline of the overlaying square laser incisions could be seen on the surface of the brain, and this was used as a reference point for the positioning of the 2 local field potential (LFP) electrodes, one of which was also used for ictogenesis. The LFP/4-AP glass electrode was placed directly in the center of cube of partially isolated brain, while the second LFP-saline electrode was placed about 2 mm outside of the cube (Fig. 1B,C). Each of the electrodes was implanted at a depth of 350 μm below the brain surface. Electrophysiological recording at both electrodes was sustained for 50–90 min after injection in order to gather the raw data for further analysis of the initiation and propagation of seizures. The injection site was completely inside the box of the laser incision. In some experiments, the locations of the electrodes were reversed and the ictal focus/4-AP/LFP electrode was placed outside the cube with LFP-saline recording inside the cube. In another set of experiments, ictogenesis was elicited after a delay of 2 h instead of 0.5 h to minimize the impact of acute trauma to the cortex. A 2-h delay has been previously shown to allow partial recovery of neuronal tissue after ablation damage (Cianchetti et al. 2013). In sham, control experiments, a craniotomy was performed and ictogenesis and electrophysiology were performed after a delay of 0.5 h without performing transections. In these experiments, the LFP/4-AP electrode was positioned at a location with little surface vasculature, and the LFP-saline electrode was placed about 2 mm away.

Evaluation of Cortical Sensory Processing

In order to evaluate the functionality of the transected cortex for processing normal physiological information, peripherally triggered somatosensory responses were recorded from within the partially isolated transected cube of brain tissue. In these experiments, a metal ball electrode, connected to a micromanipulator, was positioned above the tail somatosensory region of the cortex and lowered onto the surface of the brain. Two 25-gauge needles were placed about a centimeter apart through the skin of the animal's tail connected to an isolated pulse stimulator (Model 2100 A-M System). Ten tail stimulations, each delivering 3 current pulses (1–2 mA, 1.00 s train burst width, 0.15 s pulse duration, 0.45 s interpulse period), were given at regular intervals ranging from 1 to 2 min. The ball electrode was moved through multiple locations on the cortical surface while delivering current pulses through the tail and watching for positive responses to stimulation. The area that produced the highest amplitude and proportion of spike responses when stimulated was chosen as the designated tail somatosensory region. Immediately before the ball electrode was retracted, an image of the electrode's precise placement was taken under the magnification of the light microscope as a reference point for in vivo imaging.

Once the topographical map of tail somatosensory region was constructed using known stereotactic coordinates (Carol 1976; Yen and Chen 2008), in vivo imaging and laser microtransection therapy steps were carried out, with the only difference being that in these animals, the imaging beam and thus the ablation cutting program as well, were positioned precisely over the previously designated tail somatosensory region, regardless of surface vasculature. This guaranteed that the 3D cube of laser incisions was surrounding the cortical column containing the tail somatosensory responses. The size of the isolated area was more or less arbitrary, but based on empirical estimates of the size of the 4-AP seizure focus using imaging and electrophysiology (Zhao et al. 2011; Liou et al., 2018). After completion of the microtransections, tail stimulation was repeated using the same tail electrodes and stimulation parameters after repositioning the ball electrode on the cortical

surface within the confines of the partially isolated cortical cube of tissue containing the tail somatosensory column.

Postmortem Histology

Formaldehyde-fixed sections (30 μm) from brains were prepared as described previously (Nguyen et al. 2011). Transverse and coronal sections in different animals were done to evaluate the completeness and uniformity of the laser incisions around all 4 sides in different planes and depths (Fig. 1D). The sections were stained with diaminobenzidine (DAB; Vector: Peroxidase Substrate Kit) and hematoxylin and eosin (H&E) using standard protocols to view the red blood cells surrounding the laser incisions (DAB), and the nuclei and cytoplasm of the neurons (H&E), respectively. In order to measure the cutting width and cutting box, serial sections ranging in depth from 150 to 750 μm beneath the cortical surface were imaged in a subset of animals using bright field microscopy on a Zeiss Axio Examiner D1 with a Zeiss 10×/0.3NA lens. Widths were measured 5 times per slice and averaged for each slice of each brain by ImageJ.

Fluorescamine Imaging of 4-AP Diffusion

In order to characterize the radial diffusion pattern of 4-AP, we combined the 4-AP with fluorescamine, a fluorescent agent that reacts with primary amines to form a highly fluorescent compound (Nakai et al. 1974; Funk et al. 1986; El-Fatary et al. 2013). Serial imaging of the fluorescence of the mixture of fluorescamine and 4-AP can be used to trace the diffusion of 4-AP over time. After the same craniotomy described above, the same single-barreled glass microelectrode was loaded with fresh mixed fluorescamine/4-AP solution (25 mM 4-AP and 270 mM fluorescamine, Sigma). A 0.5 μL fluorescamine/4-AP solution was injected into neocortex at a 45°-angle using a Nanoject injector (Drummond). We excited fluorescamine/4-AP with a 395 nm LED light (M395L3, Throlabs) passed through a 395 ± 2 nm bandpass filter. The excitation light was diverted onto the neocortex via an extended reflectance dichroic mirror (FF414-Di01, Semrock). The emitted fluorescence was passed through a bandpass emission filter (FF01-474/27, Semrock) and collected by an Adimec 1000 M/D camera. Images were binned 3 × 3 and acquired every 10 s over a 2-h duration (Imager 3001, Optical Imaging Inc.) for 1 s.

Data Analysis

The offline analysis was performed using custom analysis software written in Matlab (MathWorks). Determination of seizure onset, duration, amplitude, and power were performed by visual recognition of seizure onset and termination time points, according to the characteristics outlined by Zhao et al. (2011). The electrophysiology recordings from LFP/4-AP and LFP-saline electrodes were analyzed blindly by 4 separate individuals to avoid biased scoring. Then, the seizures identified from each trace were matched together according to their time of occurrence. Seizures identified in the LFP/4-AP trace that were not identified in the LFP-saline trace were scored as seizures that did not propagate. Seizure onset and termination times were also determined from visual analysis, and these values were used to analyze various seizure attributes. Duration of seizures was obtained by calculating the difference between the onset and termination time points of individual seizures, maximum amplitude squared of seizures was calculated by squaring the voltage at each time point within individual seizures and then selecting the highest spike voltage, and power of seizures was calculated by integrating the area under the curve for squared voltages over time using the trapezoidal rule (Brown et al. 2014; Fritsch et al. 2014) (Fig. 3A). Periodic bursts of activity related to burst suppression interacting with interictal excitation induced by isoflurane or 4-AP were not further analyzed.

For tail stimulation experiments, a different form of analysis was used since there was no ictogenesis in these animals. The response spikes to each current pulse delivered during tail stimulation (both before and after laser incisions were made) were scored using a binary approach, with the typical biphasic form of neural response being accepted as a positive response. Then, the negative maximum amplitude of each accepted response spike was recorded and averaged across sessions depending on whether tail stimulation was given before or after laser ablation therapy.

For the fluorescamine/4-AP experiment, the relative change in fluorescence ($\Delta F/F$) for each frame was calculated at every 10 s as $(F_i - F_0)/F_0$, where F_0 is the background frame measured 10 s prior to the injection, and F_i the fluorescence value for the ith frame of the measurement. The diffusion of solution was calculated as the fluorescence above 2 standard deviation (SD) baseline activity. Baseline activity was measured from a background frame, 10 s prior to the injection. The averaged diffusion distance of each animal was measured as the mean of the distance between the maximum positive fluorescence position and the tip of glass electrode following 5 polar lines at 90°, 135°, 180°, 225°, and 270° indicated by the direction of the electrode axis.

For all data, statistical significance was determined with Student's t-test or ANOVA and post hoc tests. All data were expressed as means ± SD.

Data and Code Availability

Data and Matlab codes that support the findings of this study are available from the corresponding author upon reasonable request.

Results

Microinjection of 0.5 μL of 25 mM 4-AP elicited focal seizures that initiated at the site of injection. The characteristics of the seizures obtained in this study were identical to those described in previous publications (Schwartz and Bonhoeffer 2001; Bahar et al. 2006; Ma et al. 2009; Zhao et al. 2011). Microtransections were placed around the ictal focus in a total of 20 animals. Average cut widths varied from 157.82 ± 18.02 μm at the starting depth of 150 μm beneath the cortical surface and gradually decreasing to about 89.19 ± 10.04 μm at depths of 500 μm. Compared with the laser incision damaged wall, average box width varied from 558.47 ± 65.09 μm at the starting depth of 150 μm and gradually increasing to 704.80 ± 42.08 μm at depths of 500 μm. Overall, cut widths varied as a function of depth becoming wider towards the surface of the brain.

Femtosecond Laser Microincisions Surrounding the Focus Impair Ictal Initiation

In order to investigate the efficacy of our femtosecond laser at preventing ictal initiation we compared the frequency of ictal events between transected and control animals. In 4 animals (20%) with microtransections, all seizure initiation was abolished, whereas this did not occur in any sham animals (Fig. 2B). In the remaining 16 animals, there was a 63.3% reduction in the number of seizures with 119 events (n = 7.44 ± 4.02 events/animal) compared with 223 events in 11 sham animals (n = 20.27 ± 9.76 events/animal)

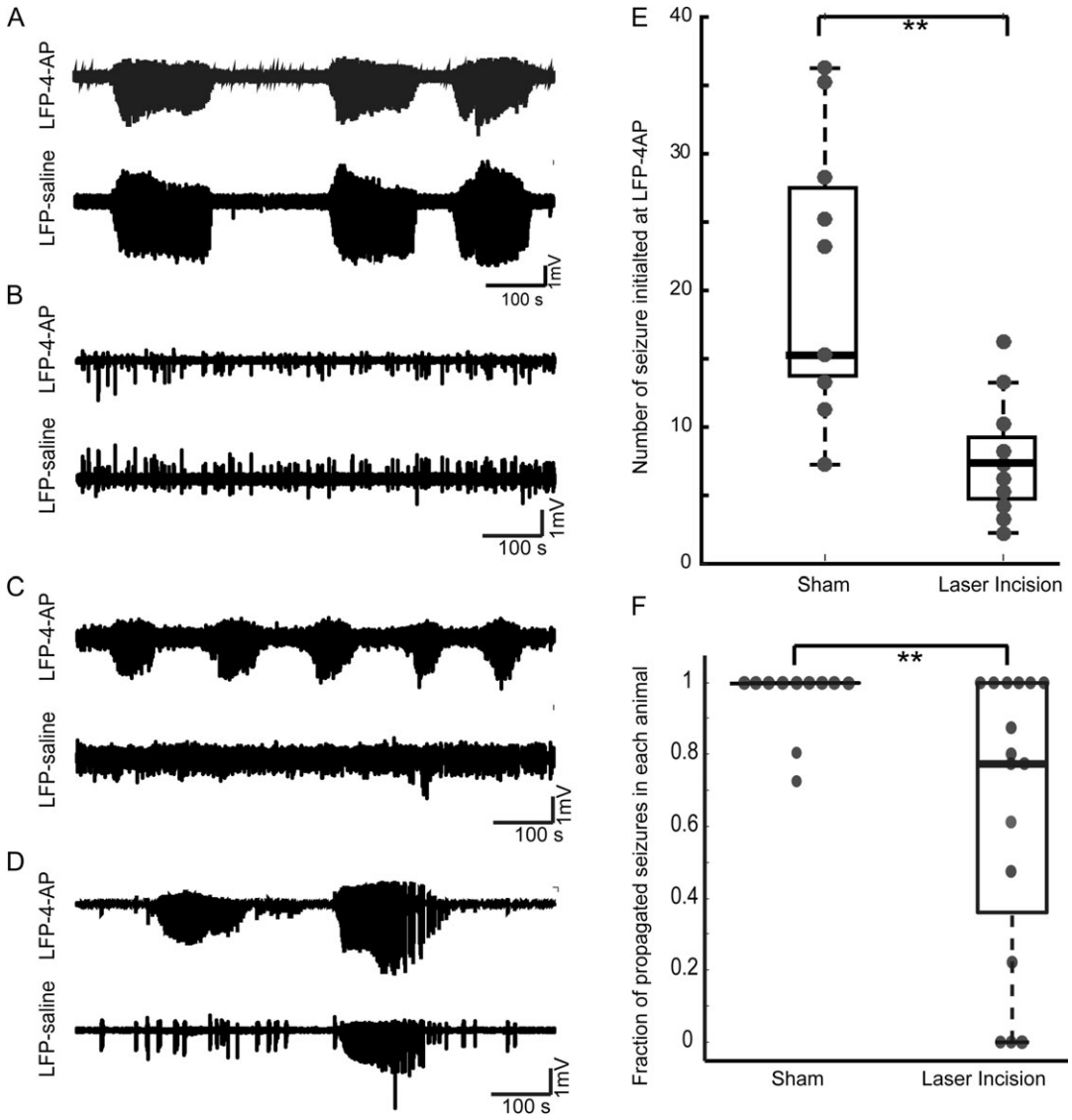

Figure 2. Laser incisions reduce the percentage of ictal events that initiate and propagate. (*A*) LFP traces from a representative sham (control) animal showing normal propagation of seizure from LFP/4-AP to LFP-saline electrodes. (*B*) LFP trace from a transected animal showing no seizure initiation at the LFP/4-AP electrode. (*C*) LFP traces from a representative microtransected animal showing complete blockage of seizure propagation from LFP/4-AP to LFP-saline. (*D*) LFP trace from a microtransected animal showing partial blockage of seizure propagation from LFP/4-AP to LFP-saline electrodes. (*E*) Femtosecond laser microtransections impair ictal initiation measured as number of seizures per animal (*t*-test, $P < 0.005$). (*F*) In microtransected animals ($n = 16$), the percentage of seizures that propagate from LFP/4-AP to LFP-saline was significantly reduced by 36.13 % when compared with sham animals ($n = 11$, *t*-test, $P < 0.05$). (*$P < 0.05; **$P < 0.01$; ***$P < 0.001$.)

(Fig. 2E; *t*-test, $P = 0.0013$). Animals in which there was no ictal initiation were not included in any other data analysis that followed as they did not contribute information to the efficacy of our laser ablation therapy with regards to propagation. These results suggest that laser microtransections that isolate a 0.366 mm^3 column may be sufficient to completely block a proportion of ictal events from initiating, presumably by inhibiting the recruitment of the critical number of neurons needed to initiate a seizure.

Femtosecond Laser Microincisions Surrounding the Focus Impair Ictal Propagation

To investigate the efficacy of our femtosecond laser at preventing ictal propagation, we scored whether individual seizures that initiated at the LFP/4-AP electrode propagated to the LFP-saline electrode. In sham animals in which no laser incisions were made, 97% of the seizures induced within the isolated focus at the LFP/4-AP electrode propagated to the LFP-saline electrode location (Fig. 2A,F; 11 animals). After enclosing the seizure focus with a cube of femtosecond laser microtransections, the percentage of seizures that propagated, in those animals where seizures initiated ($n = 16$) was significantly reduced by 36.1%. (Fig. 2F; unpaired 2-sample *t*-test, $P = 0.02$). In 3 out of 16 animals (18.75%) with laser incisions, there was complete blockage of seizure propagation, in 7 animals a reduced fraction of seizures propagated, while in the remaining 6 animals all initiated seizures propagated. (Fig. 2C,D,F).

Femtosecond Laser Microincisions Surrounding the Focus Delay Ictal Propagation

For those seizures that propagated, the time interval between the LFP/4-AP electrode and the LFP-saline electrode was significantly delayed compared with the propagation delay in sham

animals (Fig. 3B; $P = 5\times10^{-5}$, ANOVA). The mean seizure propagation delay in animals with laser incisions was 8.5 ± 30 s (n = 76 seizures) and the mean in sham animals was −0.034 ± 3.6 s (n = 223 seizures).

Femtosecond Laser Microincisions Impact Seizure Duration and Amplitude

Not only did microtransections block initiation and impair propagation in a significant proportion of animals, but in those animals in whom seizures still initiated and still propagated, there were clear changes in seizure amplitude, power and duration. We hypothesized that although the laser incisions may not have blocked the propagation or initiation of all the seizures induced, they may have sufficiently attenuated the seizures to an extent that could be therapeutic. We first measured the impact of the transections on the events recorded at the seizure initiation site, the LFP/4-AP electrode. The attributes were compared between 3 groups: sham animals (n = 11 animals; n = 223 seizures), animals with laser incisions that propagated (prop; n = 13 animals; n = 76 seizures) and that did not propagate (no prop; n = 3 animals; partial no prop, n = 7 animals; n = 43 seizures).

The mean maximum amplitude squared of seizures recorded at the initiation site was reduced in all transected animals. Compared with sham animals (18 ± 16 mV^2), amplitude was reduced by 79.4% for seizures that did not propagate (3.7 ± 15 mV^2) and by 51.1% for seizures that propagated (8.8 ± 15 mV^2) (Fig. 3C; ANOVA, P = 0.0001; Tukey's HSD, sham vs. prop: $P < 0.001$, sham vs. no prop: $P < 0.001$, prop vs. no prop: $P < 0.05$).

Seizure duration in microtransected animals was also impacted. While seizures that did not propagate were shorter than in control animals (39±41 s vs. 52±25 s), microtransected animals whose seizures propagated, surprisingly had a longer duration (81±40 s) (Fig. 3D; ANOVA, $P = 1.3\times10^{-12}$; Tukey's HSD, sham vs. prop: $P < 0.001$, sham vs. no prop: $P < 0.05$, prop vs. no prop: $P < 0.001$).

For each of the seizure attributes described, potential sources of variation apart from whether or not laser incisions were made, were identified. These included individual animals, day of experiment, and length of recording time after 4-AP injection. Statistical analysis showed that the most significant source of variation in onset delay, duration, and maximum amplitude squared of seizures at LFP/4-AP was the presence or absence of laser microtransections (ANOVA, $P = 1.1\times10^{-5}$). However, for power of seizures at LFP/4-AP, length of recording

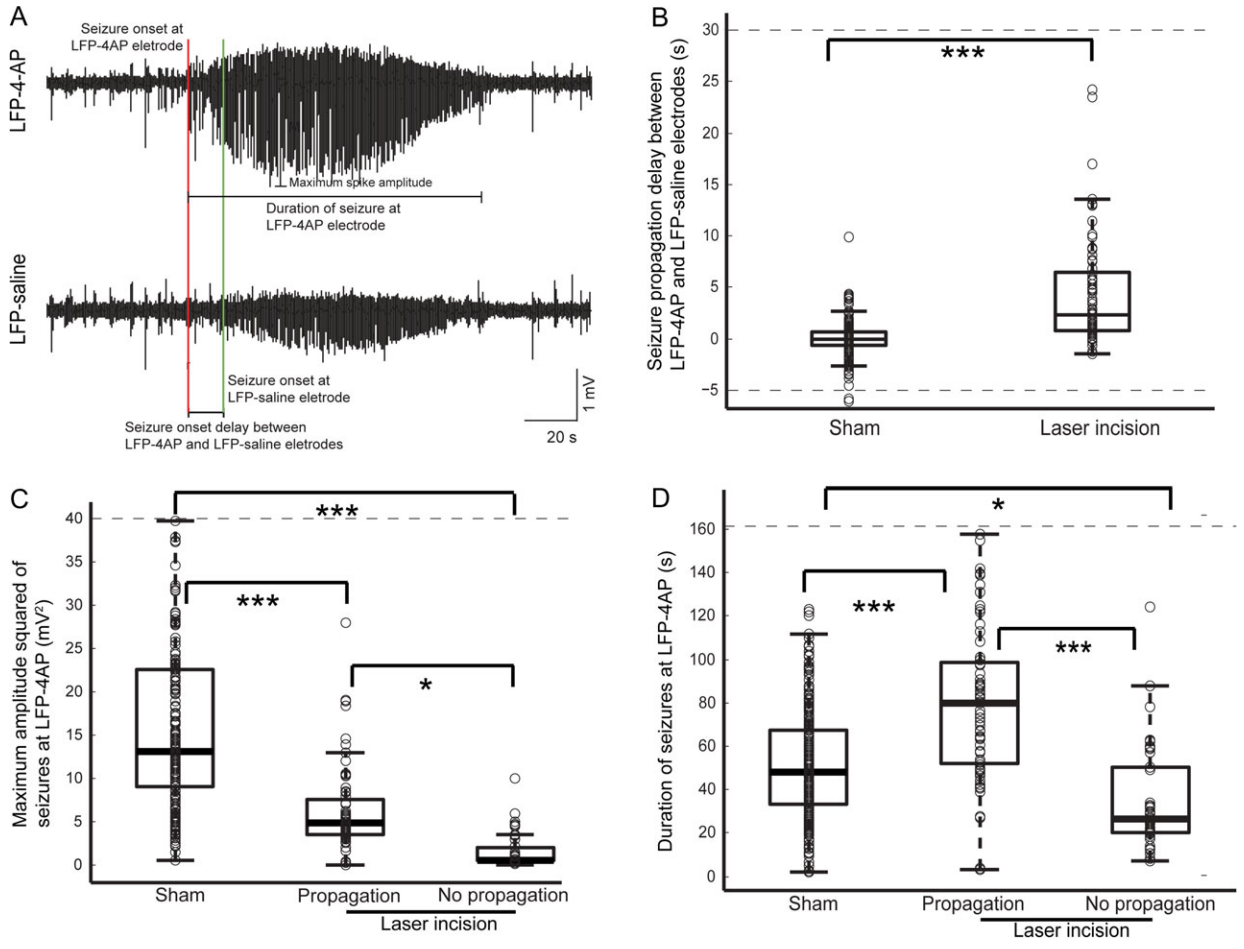

Figure 3. Microtransections alter amplitude and duration of seizures at the initiation site. (*A*) Annotated LFP traces show an example of a propagated seizure with delayed initiation. (*B*) Onset of seizures at the LFP-saline electrode was significantly delayed in animals with laser microtransections compared with sham animals ($P < 0.0001$). (*C*) Maximum amplitude squared of induced seizures, both that propagate and do not propagate in animals with laser incisions was significantly lower than the amplitude of seizures in sham animals ($P < 0.00001$). (*$P < 0.05; **$P < 0.01; ***$P < 0.001$). (*D*) Duration of seizures that did not propagate in animals with laser incisions was significantly shorter than duration of seizures in sham animals ($P < 0.005$). The seizures that do propagate in animals with laser incisions had a longer duration than seizures in sham animals ($P < 0.005$).

time after injection was also significant (ANOVA, $P = 9 \times 10^{-7}$), in addition to the presence of microtransections (ANOVA, $P = 0.005$).

To investigate the effect of microtransections on the seizure propagation, we also compared seizures characteristics at the point of propagation (LFP-saline electrode). The mean maximum amplitude squared of seizures was reduced by 33% in all microtransected animals ($5 \pm 12\,mV^2$) compared with sham animals ($15 \pm 14\,mV^2$). However, propagated seizures were longer in duration than in control animals (66±32 s vs. 50±23 s, *t*-test, $P < 0.001$) (Fig. 4).

In summary, laser microtransections completely blocked all seizure initiation in 20% of animals and completely blocked propagation in another 15% of animals. Those seizures that did not propagate also showed amplitude reductions of 79.4% and a 25% decrease in duration. In the remaining 65% of animals, seizure frequency was reduced by 63.3% compared with control animals and propagation of those seizures were completely blocked 36.1% of the time. Of the seizures that successfully initiated and propagated, there was a 51.1% reduction in amplitude at the initiation site, a 33% reduction in amplitude at the propagation site and a propagation delay of 8.5 s. However, duration of these seizures was also increased by roughly 30%.

Microtransections Attenuate but do not Block Cortical Somatosensory Impulses

To evaluate the impact of the laser cuts on normal neural function, tail somatosensory evoked responses were recorded before and after laser microtransections (Fig. 5A,B). The fraction of tail shocks that elicited a spike response before and after laser microtransections was not statistically different (84% vs. 89%) (Fig. 5C; 3 animals; $n = 90$ current pulses). However, the mean maximum amplitude of the response was reduced by 59.5% (–0.34 ± 0.15 mV) compared with before the microtransections (–0.84 ± 0.35) (Fig. 5D; 3 animals; $n = 90$ current pulses; unpaired 2-sample *t*-test; $P < 0.05$). Compared with the laser wall, the box was big enough to avoid that most of the cells inside the box were damaged. Furthermore, we did observe seizures inside the box as well as stimulus triggered LFP increases, suggesting that the presence of preserved healthy cells.

Microtransections Markedly Attenuate Propagation Into Center of Partially Isolated Cube

When the positions of LFP/4-AP and LFP-saline electrodes were reversed so that 4-AP would be injected outside of the partially isolated cortical tissue column (Fig. 6A), 28% of seizures failed to propagate into the region of isolated brain. More importantly, the power of the seizures that were recorded within the isolated focus was significantly reduced by 94.6% ($2.6 \pm 4.3\,mV^2$ s vs. $0.14 \pm 0.38\,mV^2$ s) (Fig. 6C; 3 animals; $n = 57$ seizures; unpaired 2-sample *t*-test, $P = 4 \times 10^{-5}$). Notably, although binary scoring of seizures shows that 72% of seizures propagated into the isolated cortical tissue column, the power and maximum amplitude of the seizures recorded inside the cortical tissue column were negligible (Fig. 6B).

Probability of Seizure Propagation Increases With Time

The duration of electrophysiology recording of seizures for each animal is typically 50–90 min and during this period, we observed that the probability of successful seizure propagation increased with time (Fig. 7A; 16 animals; $n = 119$ seizures; ANOVA, $P < 0.05$). One hypothesis was that the cortex was recovering from postablation tissue shock and gradually recovered during the recording period. To explore these possibilities, a set of experiments were performed where the delay between microtransections and recording was increased to 2 h versus 0.5 h to allow the tissue to recover. Not only were the earlier seizures equally well-blocked but a similar significant positive correlation was observed, indicating that tissue shock could not explain our findings (Fig. 7B; 7 animals; $n = 90$ seizures; ANOVA, $P < 0.05$).

A second hypothesis we explored was the possibility that progressive diffusion of 4-AP past the microtransections might increase propagation success. To address this issue, we investigate the in vivo diffusion distance of 4-AP by using a fluorescamine/4-AP bioassay to visualize the amounts of diffusion at different distances from the point of injection. The mixture of fluorescamine/4-AP showed strong fluorescence signals compared with the background autofluorescence of cortex (Fig. 8A). Using this method, we obtained an estimation of the distance of 4-AP diffusion in the cortical tissue. Data from individual

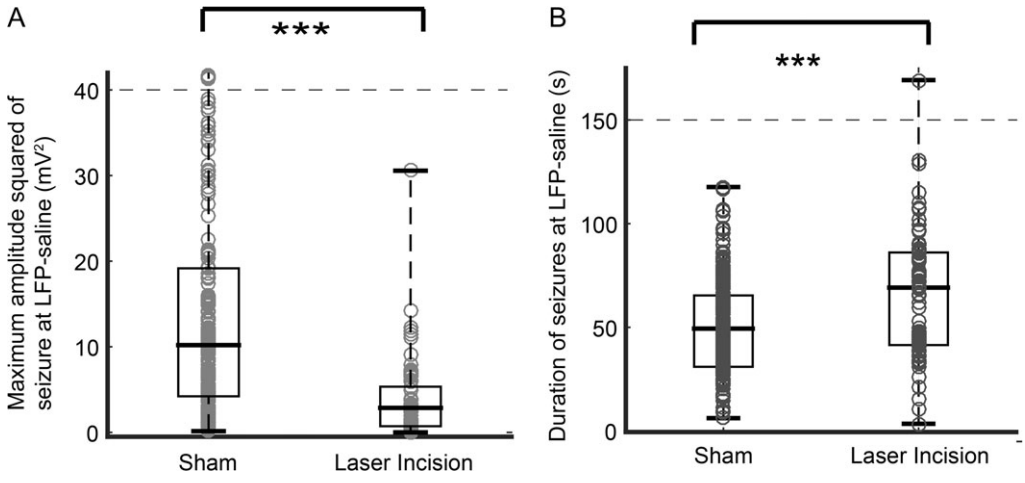

Figure 4. Microtransections alter amplitude squared and duration of seizures at the propagation site. (*A*) Maximum amplitude squared of induced seizures with laser incisions was significantly lower than the power of seizures in sham animals ($P < 0.001$). (***$P < 0.001$). (*B*) The seizures that do propagate in animals with laser incisions had a longer duration than seizures in sham animals ($P < 0.001$).

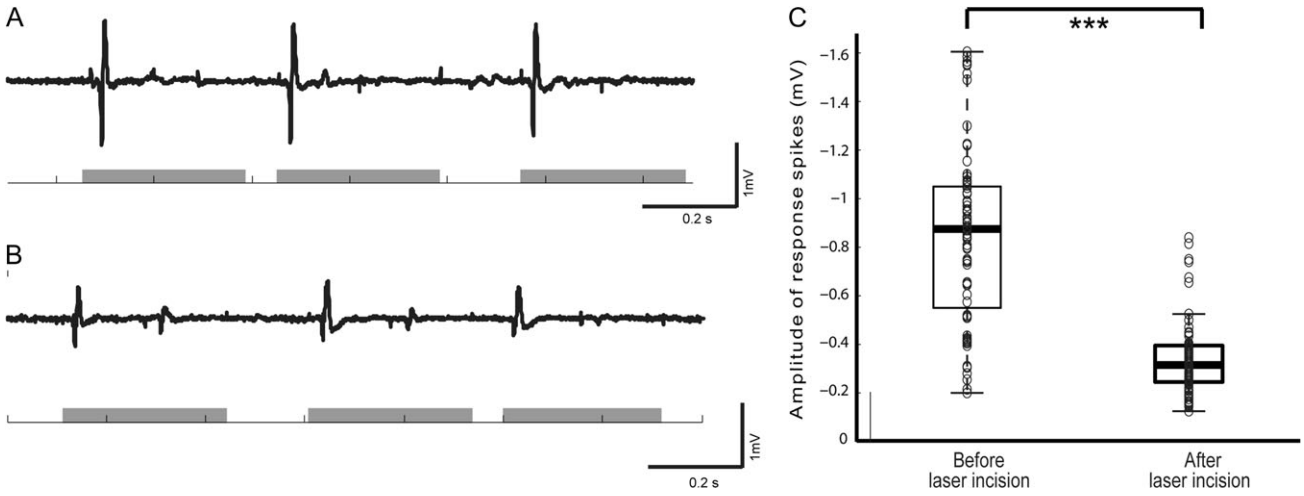

Figure 5. Somatosensory function is preserved but attenuated in animals with laser incisions. (*A*) 84.4% of current pulses (1–2 mA, 1.00 s train burst width, 0.15 s pulse duration, 0.45 s interpulse period) delivered before laser incisions were made elicited response spikes in the tail somatosensory cortex. (*B*) After laser incisions, current pulses were delivered to the same animals and 88.9% of the current pulses elicited response spikes. (*C*) The amplitude of response spikes after laser incision were measured, however, significantly smaller than the amplitude of response spikes before laser incisions. (*$P < 0.05$; **$P < 0.01$; ***$P < 0.001$.)

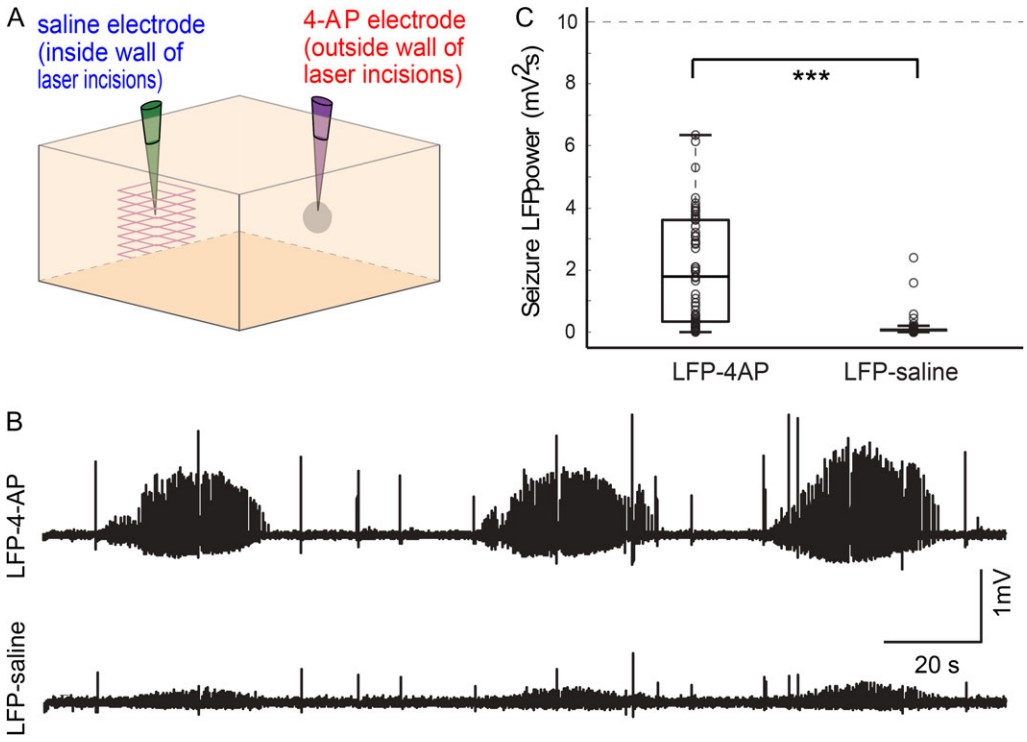

Figure 6. Microtransections markedly attenuate propagation into center of partially isolated cube. (*A*) The positions of the LFP/4-AP and the LFP-saline electrodes were reversed so that 4-AP would be injected outside of the isolated focus. (*B*) LFP trace from a representative animal shows that seizure propagation is significantly attenuated into the isolated cortical tissue. (*C*) Seizure power recorded at the LFP/4-AP electrode positioned outside of the isolated cortical tissue was significantly higher than seizure power recorded at the LFP-saline electrode positioned within the isolated cortical tissue ($P < 0.0001$). (*$P < 0.05$; **$P < 0.01$; ***$P < 0.001$.)

animals show a variation between polar lines of up to 97.3% indicating asymmetry in injection radius (Fig. 8*B*). On average, injection of 4-AP leads to an early rapid increase in the area of fluorescence with a second slower increase from diffusion (n = 5 animals). The average maximum area of diffusion of 589.60 ± 85.72 μm was reached at 3600 s (Fig. 8*C*). Considering that the length of each side of our cube of laser microtransections in the x- and y-planes was 750 μm, it is feasible that the 4-AP would diffuse past this margin within the duration of our experiments causing increased seizure propagation over time. Given the asymmetry of spread (92.69 ± 8.96%, n = 5 rats), this could result in variability in propagation success in different directions.

Discussion

In this article, we demonstrate that ~100 μm-wide femtosecond laser transections limited to supragranular layers are effective

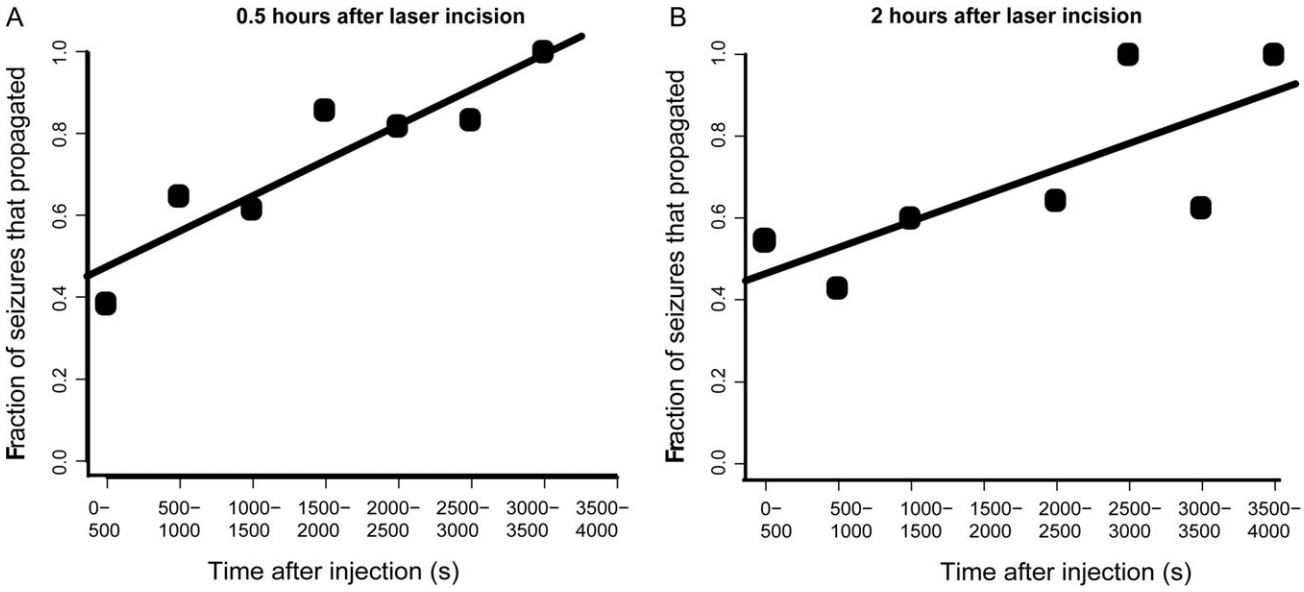

Figure 7. Seizure propagation increases over time regardless of temporal delay between transections and injection. (A) When electrophysiology recording was performed 0.5 h after laser incisions, the fraction of seizures that propagated increased with time ($P < 0.05$). (B) Delay of 2 h between microtransections and 4-AP injection resulted in similar delay over time ($P < 0.05$).

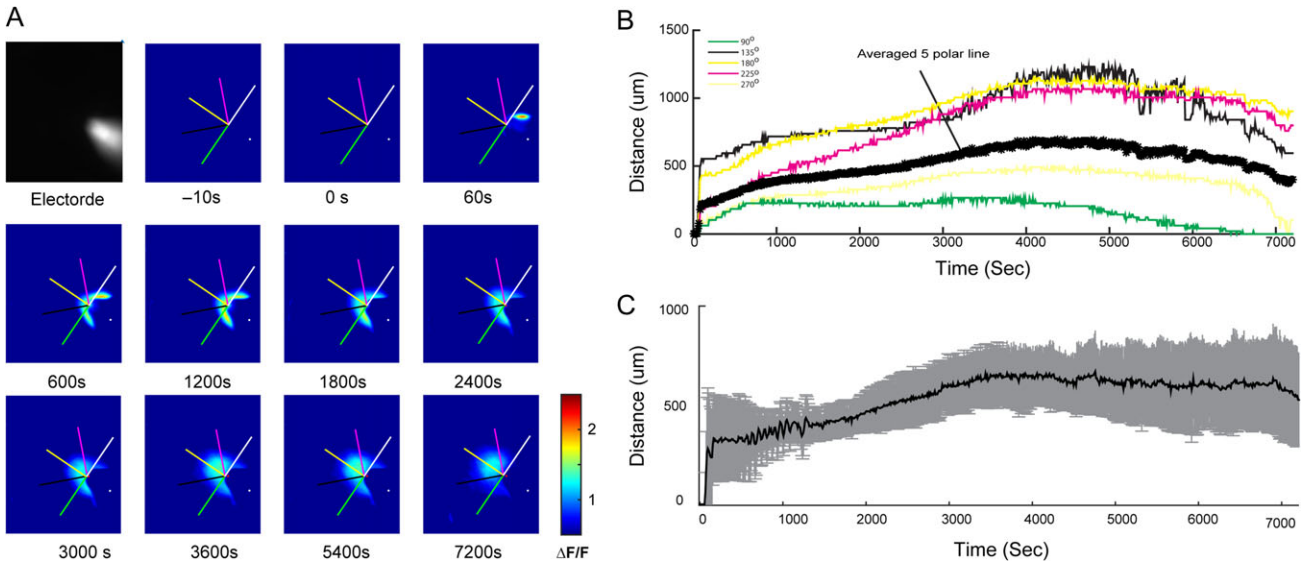

Figure 8. Diffusion of 4-AP. (A) A glass electrode loaded with fluorescamine/4-AP solution showed strong fluorescence signals inside the neocortex before injection (top left corner gray image). Fluorescence images (ΔF/F) at selected time points after 4-AP injection in a single animal presented the amounts of diffusion at different distances from the tip of injection over times. Five polar lines (at 90°, 135°, 180°, 225°, and 270° indicated by the direction of electrode axis; 2 mm) were used for estimating the 4-AP diffusion distance. The color scale-bar is shown on the last image. (B) Time course of 5 polar lines (color traces) and averaged (thick black trace) diffusion distance in a single animal. (C) Averaged 4-AP diffusion distance over 2 h after injection (SD: gray color; $n = 5$ rats).

at markedly decreasing the initiation as well as the propagation of acute focal ictal events in vivo. The technique we employ is novel not only in the limited depths of the transections, which leverages our understanding of seizure propagation, but the ability to encircle the focus with a circumferential transection "moat" rather than performing the classic linear adjacent transections done in the original description of MSTs, performed primarily to prevent initiation. Moreover, somatosensory responses are preserved with only a reduction in amplitude. Somatosensory potentials may have been attenuated based on the more limited volume of tissue activated after the transections through afferent stimulation. The use of a femtosecond laser has several advantages over other employed methods. The traditional method of using a bent blade has many limitations. The surgeon cannot determine the depth of the transections, the cuts are made without any knowledge of the sulcal pattern and so white matter is often undercut leading to deafferent/efferentation and there is significant surrounding collateral damage and trauma (Kaufmann et al. 1996). Recent use of synchrotron x-ray microbeams to transect cortex are noninvasive but produce only linear cuts and again cannot be shaped based on the anatomy of the sulci (Romanelli et al. 2012, 2015; Pouyatos et al. 2016). Using optical

methods to perform microtransections provide several sources of flexibility. Not only can the beams be shaped in width, direction and depth but simultaneous optical recording can be used for beam shaping and real-time feedback. Similar advantages have been shown for the use of femtosecond ablation in lamellar corneal surgery and penetrating keratoplasty where ophthalmologists need to create customized cut geometries that cannot be achieved by conventional blade methods (Farid and Steinert 2010).

Ictal Initiation and Propagation

The concept of seizures initiating from small regions of cortex dates back almost 50 years with the description of a minimal epileptogenic unit thought to be on the order of 12.5 mm^2 (Tharp 1971; Lueders et al. 1981). The original concept of MSTs was to prevent seizure initiation by isolating cortex into areas too small to generate seizures. Subsequent in vitro work, however, showed that ictal events could arise from areas as small as only a few hundred microns, even as few as 1000 neurons isolated to layer 5 (Connors 1984; Miles et al. 1984; Silva et al. 1991). More recent human studies have confirmed the existence of microseizures arising from small areas with a diameter of 400 μm (ranging from 0.16 to 1.76 mm^2) (Schevon et al. 2008, 2010) While seizures are thought to arise in large pyramidal cells in Layer 5, propagation has been proposed to spread preferentially through horizontal connections in layers 2/3 (Silva et al. 1991; Albowitz and Kuhnt 1995; Ulbert et al. 2004; Shipp 2007; Wenzel et al. 2017). The advantage of the 4-AP model is that inhibition is preserved, which allows us to investigate the impact of supragranular layer-specific transections with preserved inhibition in vivo. Ictal events with the 4-AP model are stereotypical, reproducible and reliable, which permits comparison between control and experimental animals with high sensitivity for an effect (Schwartz and Bonhoeffer 2001; Ma et al. 2009; Zhao et al. 2009). Using tightly focused, femtosecond infrared laser, we disrupted only the cut horizontal connections of neocortex. This highly precise disconnection attenuated the lateral horizontal spread of 4-AP induced seizures. Our results show that limited layer 2–4 microtransections are sufficient to have a dramatic impact on both seizure initiation and propagation. By limiting transection to supragranular layers, collateral damage is minimized as is the impact on normal cortical processing.

One possible mechanism for delayed but preserved seizure propagation is involvement in the thalamus (Hirata and Castro-Alamancos 2010). The corticothalamo-cortical loop has been shown to be activated in both clinically in humans and animal models of epilepsy (Gotman et al. 2005; Avoli 2012; Paz et al. 2013) and may act as a modulator of ongoing activity (Sherman and Guillery 1998; Paz and Huguenard 2015). Thus, vertical circuits may be a possible mechanism for the increased probability for the seizure breaking out with time. Other reasons for delayed propagation include infragranular propagation, which may be multisynaptic and less efficient or incomplete transections with some preserved, albeit, diminished lateral connections (see below).

Technical Limitations and Modifications

While initiation and propagation were completely blocked in some animals, in other animals only attenuation of seizure initiation and propagation was achieved. Lack of complete efficacy can be attributed to several possibilities. First is tissue inhomogeneity, such as absorption from overlying blood vessels, leading to position-dependent changes in laser energy at the focus that affects the cutting process and may results in discontinuities in the transection (Horecker 1943). In fact, the dramatic increase in propagation attenuation with the reverse experiment, that is, recording electrode within the transected cube, indicates that alterations in the transection locations and morphology can increase efficacy. For example, it might be possible to make multiple concentric walls of transections or a helical spiral or a second outer transection limited to infragranular layers adjacent to an inner supragranular transection. The current laser technology which are available in our lab cannot reliably produce cuts at depths of greater than ~800 μm. However, with longer wavelength lasers, which are now becoming available, we would be able to cut to depths of nearly 3 mm. The human implementation would be feasible in the near future using those longer wavelength lasers. The specific design and performance of the transections could be performed robotically and tailored to the patent's specific cortical anatomy and seizure focus.

Relevance to Human Epilepsy

The 800 nm light source used in this study can theoretically penetrate up to 2 mm below the brain surface; however, with a 1300 nm light source, up to 4.8 mm below the brain surface could be achieved (Nguyen et al. 2011), which is more than enough to transect the full 2.6 mm depth of human gray matter (DeFelipe et al. 2002). Furthermore, a miniaturized probe could be developed for femtosecond laser microsurgery and 2-photon imaging in the human as well as a neuroendoscope for transected deep structures such as the hippocampus (Hoy et al. 2008). This technique could also be applicable to lesional epilepsy or focal cortical dysplasia by circumscribing the lesion with a similar supragranular transection. However, transection depth and laser strength would have to be investigated for different pathological entities.

Although our transections only completely blocked seizures in 1/3 of rats, these results are more impactful than currently utilized surgical techniques in humans such as vagal nerve stimulation, deep brain stimulation and responsive neurostimulation, which only decrease seizure frequency by ~50% in association with anticonvulsant medications (Dalkilic 2017). Variability in drug diffusion, depth of anesthesia and stochastic ictal initiation may explain the lack of homogeneity in our results.

In conclusion, we have shown that limited supragranular laser microtransections are extremely effective at attenuating ictal initiation and propagation in an acute rodent seizure model. Moreover, modifications in transection morphology and depth could further improve efficacy. In combination with anticonvulsant medication, such a technique, adapted for human use, could have a profound impact on patients with epilepsy with limited side effects.

Funding

National Institute of Neurological Disorders and Stroke R01 NS49482 (T.H.S.), the American Epilepsy Society seed grant (T.H.S.), the National Institute of Neurological Disorders and Stroke R21 NS078644-01A1 (C.B.S. and T.H.S.), the Clinical Translational Science Center (CTSC), National Center for Advancing Translational Sciences (NCATS) grant UL1 RR 024996 Pilot (M.Z. and C.B.S.), the Cornell University Ithaca-WCMC

seed grant (M.Z. and C.B.S.), and the Daedalus Fund for Innovation (T.H.S, C.B.S, and M.Z.).

Notes

We would like to acknowledge Rafael Yuste, MD, PhD, who originally helped conceive of this idea in 1996. *Conflict of interest*: The authors declare a potential conflict of interest. The devices and methods presented in this manuscript are protected by patent applications.

References

Albowitz B, Kuhnt U. 1995. Epileptiform activity in the guinea-pig neocortical slice spreads preferentially along supragranular layers-recordings with voltage-sensitive dyes. Eur J Neurosci. 7:1273–1284.

Avoli M. 2012. A brief history on the oscillating roles of thalamus and cortex in absence seizures. Epilepsia. 53:779–789.

Bahar S, Suh M, Zhao M, Schwartz TH. 2006. Intrinsic optical signal imaging of neocortical seizures: the 'epileptic dip'. Neuroreport. 17:499–503.

Benbadis SR. 2001. Epileptic seizures and syndromes. Neurol Clin. 19:251–270.

Brown EC, Muzik O, Rothermel R, Juhász C, Shah AK, Fuerst D, Mittal S, Sood S, Asano E. 2014. Evaluating signal-correlated noise as a control task with language-related gamma activity on electrocorticography. Clin Neurophysiol. 125:1312–1323.

Carol W. 1976. Receptive fields of barrels in the somatosensory neocortex of the rat. J Comp Neurol. 166:173–189.

Chang BS, Lowenstein DH. 2003. Epilepsy. N Engl J Med. 349: 1257–1266.

Cianchetti FA, Kim DH, Dimiduk S, Nishimura N, Schaffer CB. 2013. Stimulus-evoked calcium transients in somatosensory cortex are temporarily inhibited by a nearby microhemorrhage. PLoS One. 8:e65663.

Connors BW. 1984. Initiation of synchronized neuronal bursting in neocortex. Nature. 310:685–687.

Dalkilic EB. 2017. Neurostimulation devices used in treatment of epilepsy. Curr Treat Options Neurol. 19:7.

DeFelipe J, Alonso-Nanclares L, Arellano JI. 2002. Microstructure of the neocortex: comparative aspects. J Neurocytol. 31: 299–316.

Devinsky O, Perrine K, Vazquez B, Luciano DJ, Dogali M. 1994. Multiple subpial transections in the language cortex. Brain. 117:255–265.

Duncan JS, Sander JW, Sisodiya SM, Walker MC. 2006. Adult epilepsy. Lancet. 367:1087–1100.

El-Fatary HM, Hammad SF, Elagamy SH. 2013. Validated spectrofluorimetric determination of dalfampridine in its symthetic mixture and spiked human plasma through derivatization with fluorescamine. J Anal Tech. 3:23–26.

Farid M, Steinert RF. 2010. Femtosecond laser-assisted corneal surgery. Curr Opin Ophthalmol. 21:288–292.

Fritsch B, Reis J, Gasior M, Kaminski RM, Rogawski MA. 2014. Role of GluK1 kainate receptors in seizures, epileptic discharges, and epileptogenesis. J Neurosci. 34:5765–5775.

Funk GM, Hunt CE, Epps DE, Brown PK. 1986. Use of a rapid and highly sensitive fluorescamine-based procedure for the assay of plasma lipoproteins. J Lipid Res. 27:792–795.

Gotman J, Grova C, Bagshaw A, Kobayashi E, Aghakhani Y, Dubeau F. 2005. Generalized epileptic discharges show thalamocortical activation and suspension of the default state of the brain. Proc Natl Acad Sci USA. 102:15236–15240.

Helmchen F, Denk W. 2005. Deep tissue two-photon microscopy. Nat Methods. 2:932–940.

Hirata A, Castro-Alamancos MA. 2010. Neocortex network activation and deactivation states controlled by the thalamus. J Neurophysiol. 103:1147–1157.

Horecker BL. 1943. The absorption spectra of hemoglobin and its derivatives in the visible and near infra-red regions. J Biol Chem. 148:173–183.

Hoy CL, Durr NJ, Chen P, Piyawattanametha W, Ra H, Solgaard O, Ben-Yakar A. 2008. Miniaturized probe for femtosecond laser microsurgery and two-photon imaging. Opt Expr. 16: 9996–10005.

Kaufmann WE, Krauss GL, Uematsu S, Lesser RP. 1996. Treatment of epilepsy with multiple subpial transections: an acute histologic analysis in human subjects. Epilepsia. 37:342–352.

Kobau R, Luo Y-H, Zack MM, Helmers S, Thurman DJ. 2012. Epilepsy in adults and access to care—United States, 2010. MMWR Morb Mortal Wkly Rep. 61:909–913.

Kramer MA, Cash SS. 2012. Epilepsy as a disorder of cortical network organization. Neuroscientist. 18:360–372.

Liou J-Y, Ma H, Wenzel M, Zhao M, Baird-Daniel E, Smith EH, Daniel A, Emerson R, Yuste R, Schwartz TH, et al. 2018. Role of inhibitory control in modulating focal seizure spread. Brain. 141:2083–2097.

Lueders H, Bustamante LA, Zablow L, Goldensohn ES. 1981. The independence of closely spaced discrete experimental spike foci. Neurology. 31:846.

Ma H, Zhao M, Suh M, Schwartz TH. 2009. Hemodynamic surrogates for excitatory membrane potential change during interictal epileptiform events in rat neocortex. J Neurophysiol. 101:2550–2562.

Miles R, Wong RK, Traub RD. 1984. Synchronized afterdischarges in the hippocampus: contribution of local synaptic interactions. Neuroscience. 12:1179–1189.

Morrell F, Whisler WW, Bleck TP. 1989. Multiple subpial transection: a new approach to the surgical treatment of focal epilepsy. J Neurosurg. 70:231–239.

Mountcastle VB. 1997. The columnar organization of the neocortex. Brain. 120:701–722.

Nakai N, Lai CY, Horecker BL. 1974. Use of fluorescamine in the chromatographic analysis of peptides from proteins. Anal Biochem. 58:563–570.

Nguyen J, Ferdman J, Zhao M, Huland D, Saqqa S, Ma J, Nishimura N, Schwartz TH, Schaffer CB. 2011. Sub-surface, micrometer-scale incisions produced in rodent cortex using tightly-focused femtosecond laser pulses. Lasers Surg Med. 43:382–391.

Paz JT, Davidson TJ, Frechette ES, Delord B, Parada I, Peng K, Deisseroth K, Huguenard JR. 2013. Closed-loop optogenetic control of thalamus as a tool for interrupting seizures after cortical injury. Nat Neurosci. 16:64–70.

Paz JT, Huguenard JR. 2015. Microcircuits and their interactions in epilepsy: is the focus out of focus? Nat Neurosci. 18:351.

Pondal-Sordo M, Diosy D, Téllez-Zenteno JF, Girvin JP, Wiebe S. 2006. Epilepsy surgery involving the sensory-motor cortex. Brain. 129:3307–3314.

Pouyatos B, Nemoz C, Chabrol T, Potez M, Bräuer E, Renaud L, Pernet-Gallay K, Estève F, David O, Kahane P, et al. 2016. Synchrotron X-ray microtransections: a non-invasive approach for epileptic seizures arising from eloquent cortical areas. Sci Rep. 6:27250.

Rheims S, Represa A, Ben-Ari Y, Zilberter Y. 2008. Layer-specific generation and propagation of seizures in slices of

developing neocortex: role of excitatory GABAergic synapses. J Neurophysiol. 100:620–628.
Ribak C, Harris A, Vaughn J, Roberts E. 1979. Inhibitory, GABAergic nerve terminals decrease at sites of focal epilepsy. Science. 205:211–214.
Romanelli P, Fardone E, Bucci D, Battaglia G, Bräuer-Krisch E, Requardt H, Le Duc G, Bravin A. 2015. Microradiosurgical cortical transections generated by synchrotron radiation. Phys Med. 31:642–646.
Romanelli P, Striano P, Barbarisi M, Coppola G, Anschel DJ. 2012. Non-resective surgery and radiosurgery for treatment of drug-resistant epilepsy. Epilepsy Res. 99:193–201.
Schevon CA, Goodman RR, McKhann GJ, Emerson RG. 2010. Propagation of epileptiform activity on a submillimeter scale. J Clin Neurophysiol. 27:406–411.
Schevon CA, Ng SK, Cappell J, Goodman RR, McKhann GJ, Waziri A, Branner A, Sosunov A, Schroeder CE, Emerson RG. 2008. Microphysiology of Epileptiform Activity in Human Neocortex. J Clin Neurophysiol. 25:321–330.
Schramm J, Aliashkevich AF, Grunwald T. 2002. Multiple subpial transections: outcome and complications in 20 patients who did not undergo resection. J Neurosurg. 97:39–47.
Schwartz TH, Bonhoeffer T. 2001. In vivo optical mapping of epileptic foci and surround inhibition in ferret cerebral cortex. Nat Med. 7:1063–1067.
Sherman SM, Guillery RW. 1998. On the actions that one nerve cell can have on another: distinguishing “drivers” from “modulators”. Proc Natl Acad Sci U S A. 95:7121–7126.
Shipp S. 2007. Structure and function of the cerebral cortex. Curr Biol. 17:R443–R449.
Silva LR, Amitai Y, Connors B. 1991. Intrinsic oscillation of neocortex generated by layer 5 pyramidal neurons. Science. 251: 432–435.
Telfian AE, Connors BW. 1998. Layer-specific pathways for the horizontal propagation of epileptiorm discharges in neocortex. Epilepsia. 39:700–708.
Tharp BR. 1971. The penicillin focus: a study of field characteristics using cross-correlation analysis. Electroencephal Clin Neurophysiol. 31:45–55.
Treiman DM. 2001. GABAergic mechanisms in epilepsy. Epilepsia. 42:8–12.
Ulbert I, Heit G, Madsen J, Karmos G, Halgren E. 2004. Laminar analysis of human neocortical interictal spike generation and propagation: current source density and multiunit analysis in vivo. Epilepsia. 45:48–56.
Wenzel M, Hamm JP, Peterka DS, Yuste R. 2017. Reliable and elastic propagation of cortical seizures in vivo. Cell Rep. 19: 2681–2693.
Yen C-T, Chen R-S. 2008. Tail region of the primary somatosensory cortex and its relation to pain function. In: Onozuka M, Yen C-T, editors. Novel trends in brain science: brain imaging, learning and memory, stress and fear, and pain. Tokyo, Japan: Springer. p. 233–252.
Zhao M, Ma H, Suh M, Schwartz TH. 2009. Spatiotemporal dynamics of perfusion and oximetry during ictal discharges in the rat neocortex. J Neurosci. 29:2814–2823.
Zhao M, Nguyen J, Ma H, Nishimura N, Schaffer CB, Schwartz TH. 2011. Preictal and ictal neurovascular and metabolic coupling surrounding a seizure focus. J Neurosci. 31: 13292–13300.